DOI: ADD DOINUMBER HERE

Preparatory CFD Studies for Subsonic Analyses of a Reusable First Stage Launcher during Landing within the RETPRO Project

Tamas Bykerk ⋆ *and Sebastian Karl* ⋆
⋆ *German Aerospace Center (DLR)*
Bunsenstrasse 10, Goettingen, 37073
tamas.bykerk@dlr.de ·

Abstract

The RETPRO project (Validation of Wind Tunnel Test and CFD Techniques for Retropropulsion), as part of ESA's Future Launchers Preparatory Programme, aims at preparing the tools necessary for a reliable design and simulation of future launchers or spacecraft. A particular focus is assigned to vertical take-off and landing configurations using retro propulsion as part of their control concept for entry, descent, and landing manoeuvres. Wind tunnel tests and computational fluid dynamics are used to generate a comprehensive aerodynamic database, which is required for flight dynamics simulations, enabling mission and performance analyses of possible future launcher designs. Two successful campaigns analyzing the hypersonic re-entry burn phase of flight as well as the supersonic glide phase have been completed in the H2K and TMK facilities at DLR Cologne. The final phase of the RETPRO project looks to perform aerothermal tests by combusting H2/O2 during a retro burn in the subsonic VMK test section, simulating the landing environment. As was completed for the previous test campaigns, CFD reconstructions of selected tests are scheduled to evaluate the ability of RANS simulations to match the plume structure and flowfield, as well as surface pressure and heat flux measurements taken during the campaign. This paper will be primarily concerned with the CFD sensitivity studies conducted to determine the dependence of plume structure and surface measurements on factors such as grid density, combustion chamber conditions, freestream Mach number and Angle of Attack. The main finding is the large role post combustion plays on the temperature field and the location of peak heating on the model.

1. Introduction

The recent success of several commercial launchers in landing, recovering and relaunching complete main stages has renewed the interest in the study of re-usable space transportation concepts. As shown by several systems, a restriction to the recovery of the first stage and the application of retro-propulsion for landing appears to be a promising concept for low-cost, robust and flexible vehicles. Commercial launch vehicles, such as the SpaceX Falcon 9, has inspired the development of the vertical take-off and landing (VTVL) re-usable launch vehicle (RLV). The recovery of the first stage is achieved through strategic retro-propulsion burns, control surface deflections and deployable landing legs to accomplish a precision landing. The nature of this trajectory introduces complex flow topologies through a large range of Mach numbers, requiring a strong understanding of the vehicle aerodynamics, plume behaviour and vehicle stability.[1]

The recovery of the first stage booster is a complex task which relies heavily on the successful implementation of a control system. This requires engineers to have intimate knowledge of vehicle aerodynamics, the effect of control surface deflections and the use of propulsion systems for vehicle deceleration and attitude control. This data is typically consolidated in an aerodynamic database, where derivatives are compiled according to Mach number, Angle of Attack (AoA), thrust setting and control surface inclination angle. Due to the complexity and cost of gathering this data from full scale flight tests, results from high-fidelity CFD predictions play a large role in the vehicle design. These datasets are complemented by ground test results which further serve as a basis for CFD accuracy assessment and validation. A close interaction of wind tunnel based and CFD investigations enables the reduction of prediction uncertainties and extrapolation of ground test data to flight scales.

While there is substantial experience in load predictions for hypersonic capsule or winged type re-entry concepts, retro-propulsion maneuvers are a particularly challenging problem for both CFD and ground based testing. This is primarily due to the complex fluid mechanical and thermo-chemical interaction between the exhaust plumes and the free stream. During retro-propulsion phases, large parts of the vehicle are immersed in its exhaust gases. Large recirculation regions and zones of flow reversal significantly affect the heat load distribution and aerodynamic characteristics. Furthermore, the divergence of the exhaust jets at low ambient pressures gives rise to strong plume-plume interactions in the vicinity of the launcher base.

In this context, the RETPRO project aims at the further development and validation of experimental and numerical simulation techniques which are needed for the aerodynamic and aerothermal design of re-usable launch systems with retro-propulsion.[2] RETPRO is carried out under a programme of and funded by the European Space Agency - through the Future Launchers Preparatory Programme. RETPRO is one of a few studies within Europe looking at better understanding the requirements for the design of VTVL RLVs.[3,4]

This paper focuses on the presentation and discussion of preliminary steady-state numerical simulation results used for a sensitivity analysis for subonsic aerothermal tests. First an overview of the RETPRO vehicle is presented. This is followed by an introduction to the CFD methodologies. Finally the results are discussed and conclusions are drawn.

2. RETPRO Vehicle

The RETPRO vehicle is of a two stage design with a re-usable first stage. Four grid fins are used for attitude control and braking, while four retractable legs are intended for the vertical landing. The shape is presented in Figure 1. An overview of the full sized vehicle geometric properties is summarised below in Table 1.

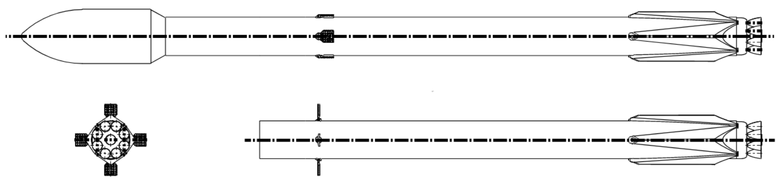

Figure 1: Overview of the RETPRO vehicle

Table 1: Geomertic properties of the full scale RETPRO vehicle

Property	**Stage 1**	**Stage 2**
Height (m)	47	23
Diameter (m)	3.66	3.66/5.20
Number of Engines	9	1

Given the harsh environment the model is subjected to during aerothermal tests, some modifications to the vehicle have been made. This includes the removal of the gridfins as well as covering the external surfaces with a copper sheath to prevent excessive heating. Images of the geometry tested can be seen in the following section, where the model is shortened and has a length of approximately 0.55m with a maximum diameter of 0.08m.

3. Methodology

3.1 Numerical Model

The TAU code is a second order finite-volume solver for the Euler and Navier-Stokes equations which includes a comprehensive range of RANS-based or scale resolving turbulence models. It uses unstructured computational grids to facilitate the analysis of complex geometries and is highly optimized for the application on massively parallel HPC systems. TAU has been successfully applied to a wide range of sub-to-hypersonic flow problems, both in scientific and industrial applications, including the analysis of re-usable launcher configurations.

The baseline set of numerical models which have been applied for the present investigations provides accurate and robust treatment for all flow conditions as defined in the CFD test matrix with a free stream Mach number of 0.8. The calculation of the inviscid fluxes in the finite volume framework is based on the application of the AUSMDV flux vector splitting scheme together with MUSCL gradient reconstruction to achieve second order spatial accuracy. Viscous fluxes are treated with a low-dissipation central discretization scheme.

Turbulence was modelled using the two equation k-ω-SST model from Menter. The single equation S-A turbulence model was found to be very effective in replicating the plume structure during the hypersonic retro-propulsion maneouvres from previous CFD reconstructions presented in refs[5,6], however it has been shown that it results in a short plume length in the subsonic regime.[7] An adequate setup of the numerical grid is required which is achieved by using prismatic sub-layers close to the wall with a first dimensionless wall spacing of y^+ in the order of one and a wall normal stretching ratio of grid cells of less than 1.3. The wall temperature was set to 300K and heat flux was assumed to be isothermal.

3.2 Internal Flow

The numerical studies which reconstruct the VMK tests required the outflow conditions at the nozzle exits to model the plume structure. The single active nozzle is powered by a combustor within the model, which is fed gaseous H2 and O2 at a oxidiser-to-fuel (O/F) ratio of 0.471 and 293 K. The combustion products are then routed through a main internal flowpath before being ejected. Nozzle exhaust has been modelled by imposing the exit flow conditions of the thrust nozzles at their respective exit planes in the computational domain of the launcher. The radial distribution of the axial and radial velocity, exit pressure and temperature was determined by separate analyses of the flow inside the thrust nozzle, which provides an accurate representation of the exhaust jet. The mass fractions and partial densities of each species from the H2/O2 combustion were also included at the nozzle outflow. The NASA CEA tool was used to determine the mass fractions at the exit of the combustion chamber, which was fed into the Tau simulations as a reservoir boundary condition. The results showing the nozzle flow for the VMK configuration are presented below in Figure 2.

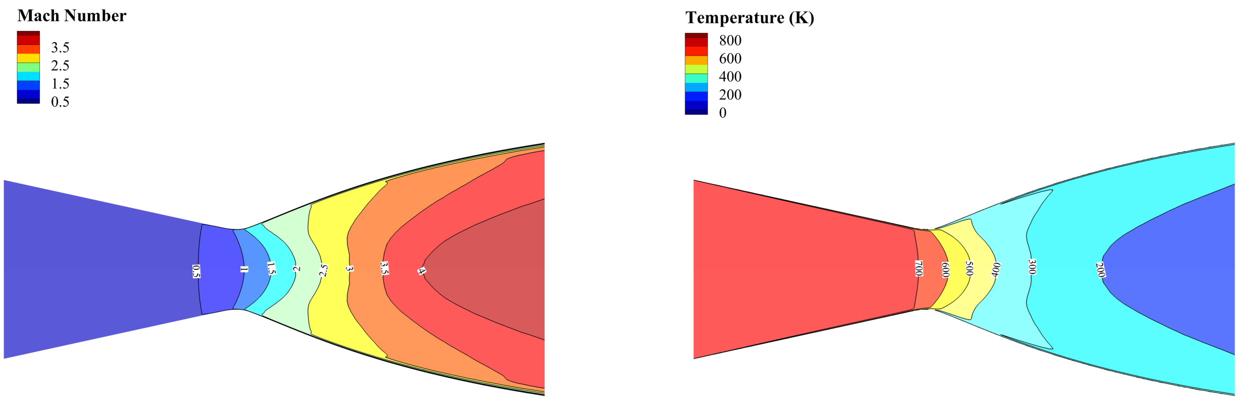

(a) (b)

Figure 2: Sample 2D nozzle solution for the VMK operating condition showing results from chemically reacting simulations for (a) Mach distribution and (b) temperature distrubution

The flow is characterised by a low temperatures, which is the result of flow expansion and lack of combustion due to the 0.471 oxidiser-to-fuel ratio and the equillibrium assumption for the combustion chamber. This means the oxygen is completely burned in the combustion chamber, causing only residual fuel and H2O to be present in the thrust nozzle. These mass fractions do not change through the nozzle path due to the lack of O2 and results in large amounts of unburned H2 to be ejected from the nozzle with a mass fraction of around 0.6.

3.3 External Flow

External flow simulations were conducted using both 2D and 3D grids. 2D axisymmetric computations were used for the tests conducted using the model without peripheral nozzles. This was aided by the nozzle of VMK, which was also modelled, has a circular cross section and is ideally suited to an axisymmetric computation, as well as the lack of fins and landing legs on the model itself. The test cases with peripheral nozzles and 0 degrees AoA were modelled using a quarter grid, while the 10 degrees AoA case was conducted using a half grid. Examples of Both 2D and 3D configurations are presented below in Figure 3. Note that the extremities of the domain are not representative of the VMK chamber size and are a farfield boundary condition. This allows air and exhaust gases to flow in and out of the domain, neglecting the influence of the walls. To reduce the point count of the grid, the model support infrastructure was removed from the CAD file. This is because the investigations are primarily focussed on the flow at the rocket nozzle exit and the influence on base heating. Given that the model mounting strut is sufficiently aft of the base area, the assumption is that its absence will have no bearing on the base flow. Additionally, limited grid refinement was placed in the wake region behind the model as no drag measurements were taken in the wind tunnel and sensor data will be located around lower portion of the model.

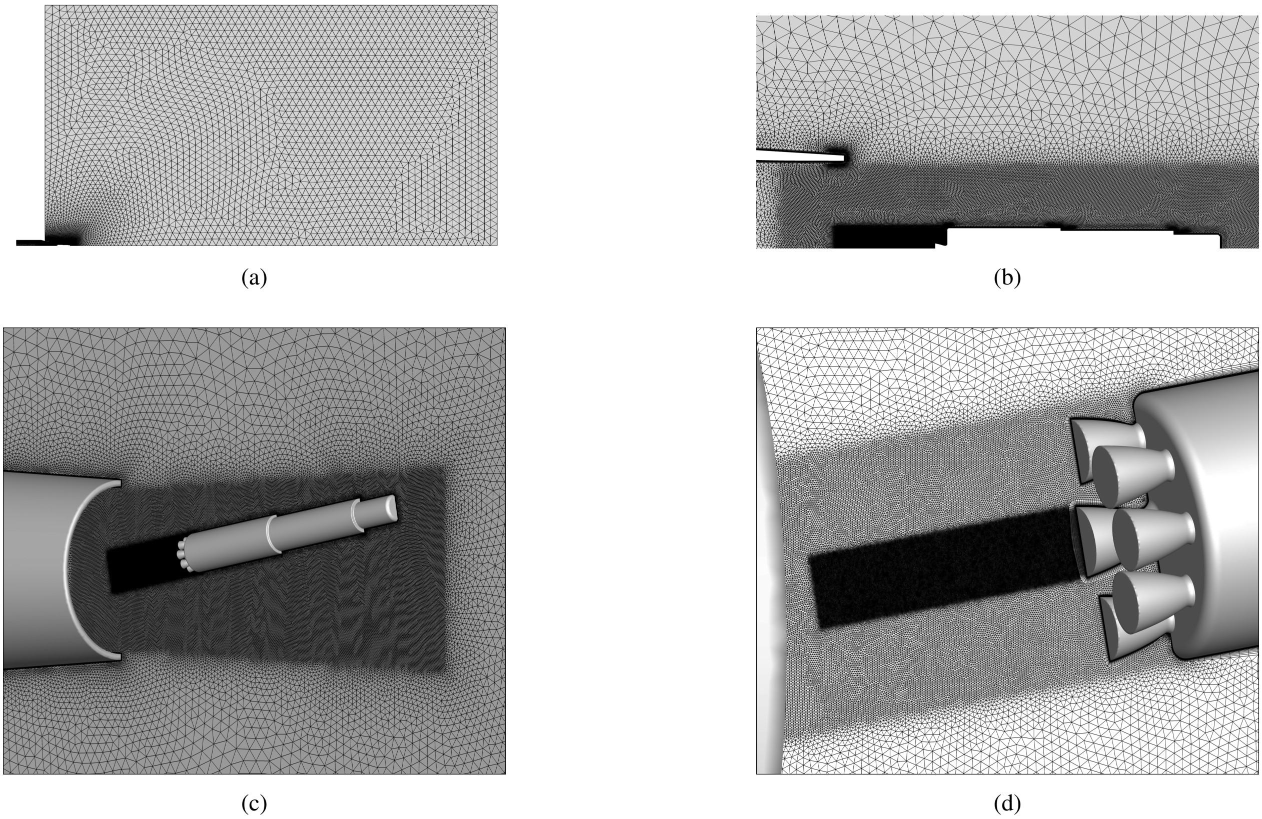

Figure 3: Views of VMK mesh showing (a) full domain, (b) closeup of nozzle and vehicle, (c) half configuration with 10 degrees AoA and (b) half configuration with 10 degrees AoA showing closeup of mesh refinement

All simulations presented here required combustion analysis and the utilisation of the non-equilibirium solver modelled the air as 22% Oxygen and 78% Nitrogen. They were determined using 9 species (H2, H, O2, O, OH, H2O, HO2, H2O2 and N2) along with the Jackimowksi 19 reaction mechanism.[8]

4. Results

4.1 Grid Density

The first investigations were to determine the influence of grid density on the plume structure. The refinement region which covers the plume and baseplate area was the only area of interest as the model will not be instrumented away from the baseplate and no force measurements will be taken during the experimental runs. This means that the flowfield downstream of the base region is not of immediate interest other than to see the exhaust gas propogation with the freestream. These investigations were completed using the 2D axisymmetric grid for the single nozzle case. The coarse grid has a refinement length scale of 0.6 mm, with each subsequent grid having this value halved such that the length scale of the finest grid was 0.075 mm. Comparisons between the four grids are shown below in Figure 4.

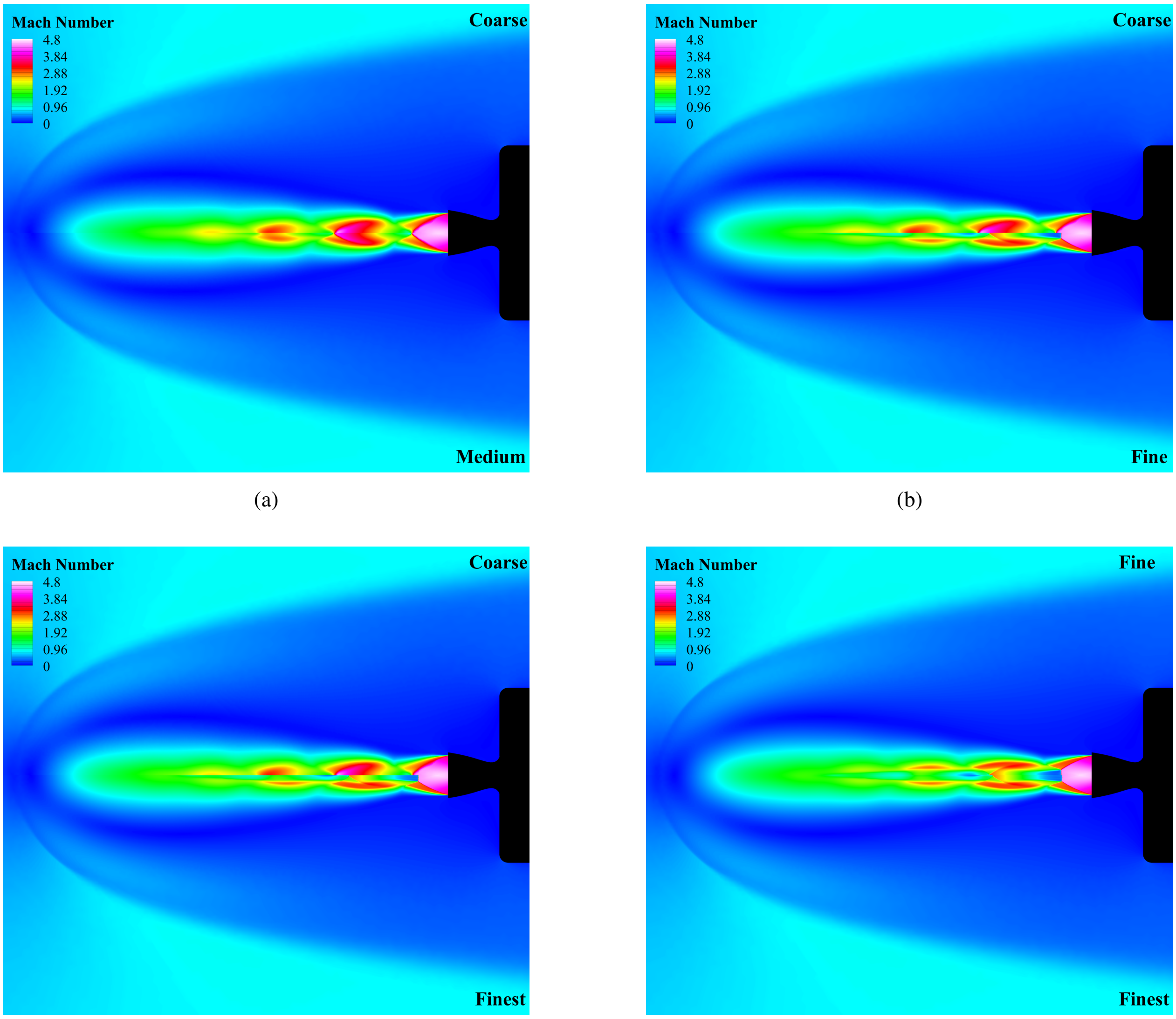

(a) (b) (c) (d)

Figure 4: Influence of grid density on plume structure showing (a) coarse vs medium, (b) coarse vs fine, (c) coarse vs finest and (d) fine vs finest grid

The difference in plume shape and structure is minimal when comparing the coarse grid with the medium grid. However, the influence of further refinement of the mesh is high, with the clear emergence of a Mach disk and trailing subsonic flow. The difference between the fine and finest grids is minimal and the plume is considered "grid converged" at the fine level. While it is important to properly resolve the plume structure for a qualitative comparison with the Schlieren photographs, it is also important to understand the variation in baseplate pressure measurements with grid density. This is because at the highest mesh density, over three quarters of the total grid points are in this refinement region and represent a noticeable increase in computational expense. As can be seen in Figure 5, the influence of grid density is minimal.

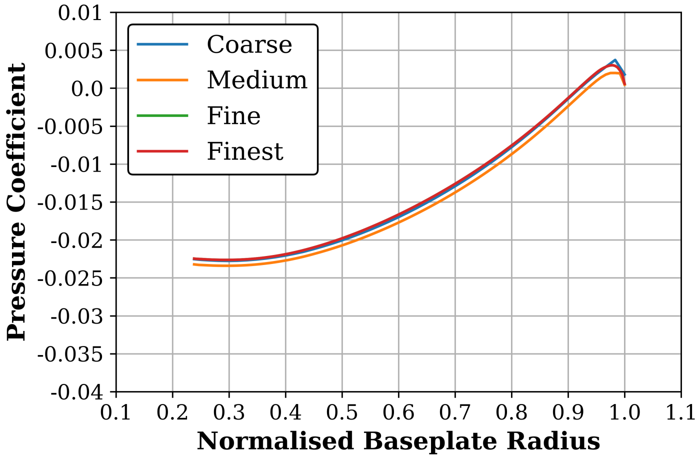

Figure 5: Comparison of base pressures for baseline, finer and finest grids

4.2 Mach Number

Figure 6 shows that for the Mach 0.5 case the plume penetration length is around 20% higher than for the Mach 0.8 case. This is because as freestream dynamic pressure increases, the plume is pushed further towards the vehicle baseplate.

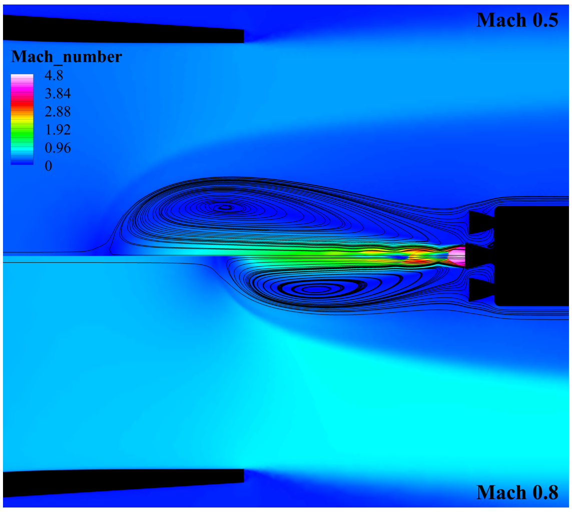

Figure 6: Comparison of flow topology between Mach 0.5 and Mach 0.8 cases

The influence of the plume structure on the base heating can be clearly seen in Figure 7, where the Mach 0.8 case sees higher heat flux. The peak heating in both cases is located around the rim of the baseplate, with the Mach 0.8 case seeing the highest heat loads in this area. The Mach 0.5 case however has more heat flow distributed around the centre of the baseplate. The way the flow interacts with the recirculation zones is a driver for the baseplate heating, with the shorter plume at Mach 0.8 directing more hot exhaust around the lip of the baseplate, with the longer plume allowing more flow to impinge the centre part of the baseplate.

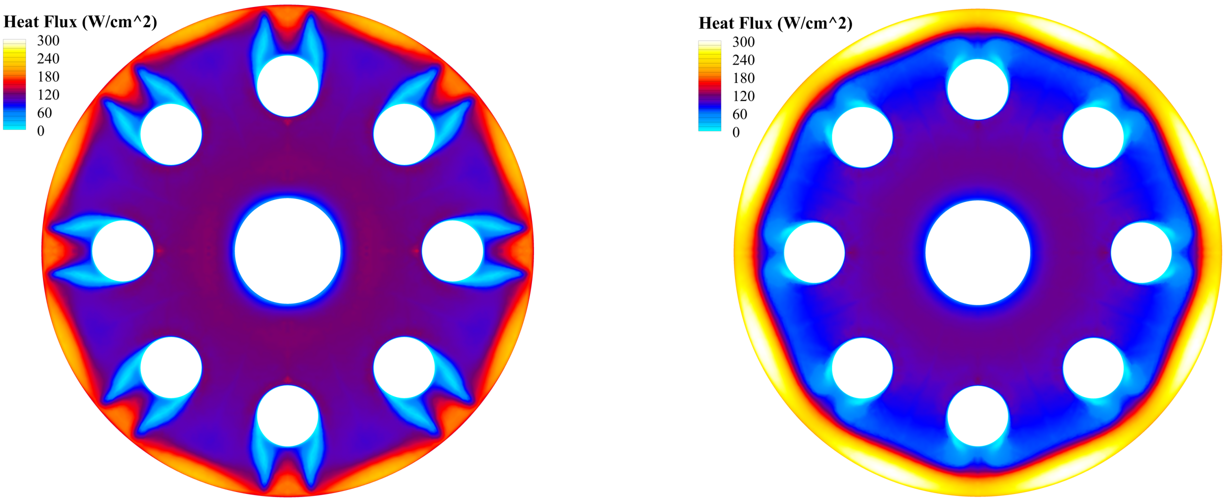

(a) (b)

Figure 7: Baseplate heatflux for (a) Mach 0.5 and (b) Mach 0.8 cases

4.3 Combustion Chamber Temperature

While the temperature of both H2 and O2 flowing into the model is known from experimental measurements, the resulting temperature in the combustion chamber is not. This was estimated to be around 750K using the NASA CEA tool which assumes equilibirum combustion. However, given the low O/F ratio, this assumption may not be entirely correct. To determine whether the combustion chamber temperature influences the base pressure coefficients, a test case was completed with the reservoir temperature set to 500K. The results from this study are presented below in Figure 8, where not only a reduction in the distance between the nozzle exit and the Mach disk is present, but also a noticeable increase in pressure coefficient and confirms the potential sensitivity of the solutions to the combustion chamber temperature.

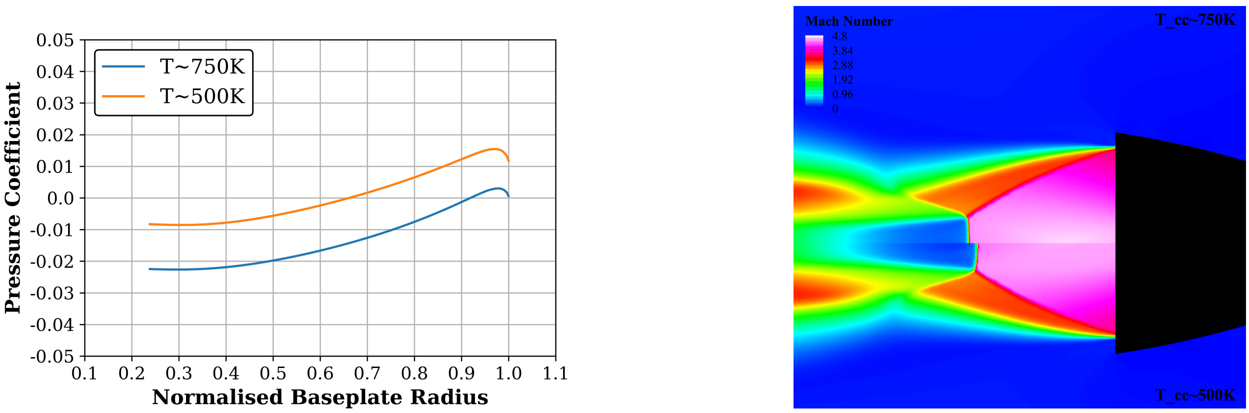

(a) (b)

Figure 8: Influence of lowering combustion chamber temperature on (a) pressure coefficient and (b) Mach disk size and location

4.4 Angle of Attack

Figure 9 contours present the outcome of the 10 degree AoA variation. The difference in the flowfield is immediately seen when compared to the baseline case. The leeward side of the model is completely immersed in the exhaust gases, while the windward side sees only impingement on the baseplate lip. The top lip of the baseplate is seen to encounter the highest heat fluxes, with a unique distribution observed elsewhere.

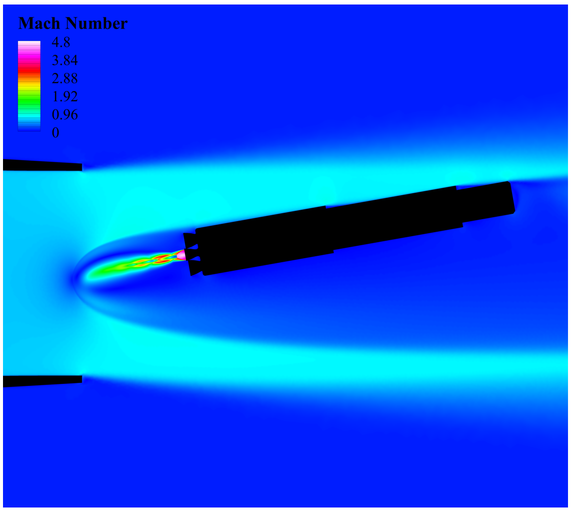

(a)

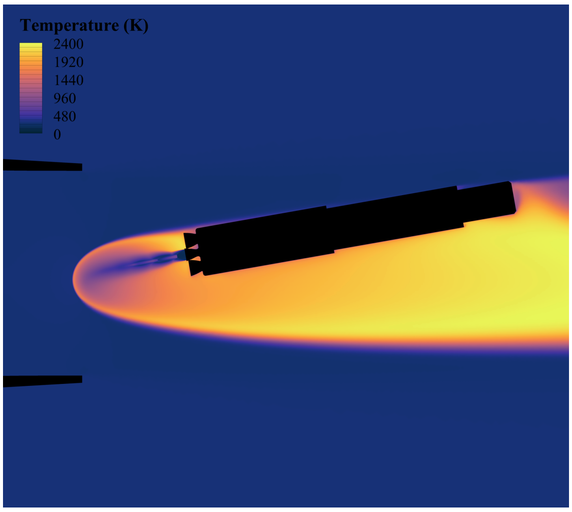

(b)

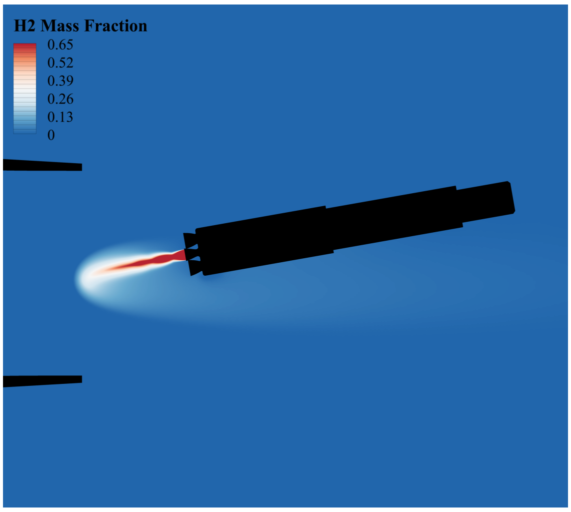

(c)

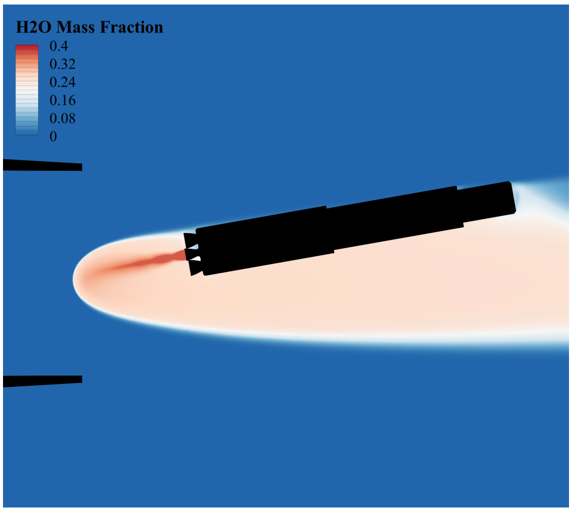

(d)

Figure 9: CFD contours for VMK Mach 0.8 case showing (a) Mach number, (b) temperature, (c) H2 mass fraction and (d) H2O mass fraction

Analysing the patterns it appears as if the hot gases are flowing top to bottom when viewing Figure 10, where the cooler regions indicate areas of flow separation underneath the nozzles. The addition of AoA to the test also results in an asymmetric flowfield, where the recirculation zone on the leeward side of the plume is smaller than that of the windward. The plume also appears to bend away from the centreline as it encounters the oncoming flow.

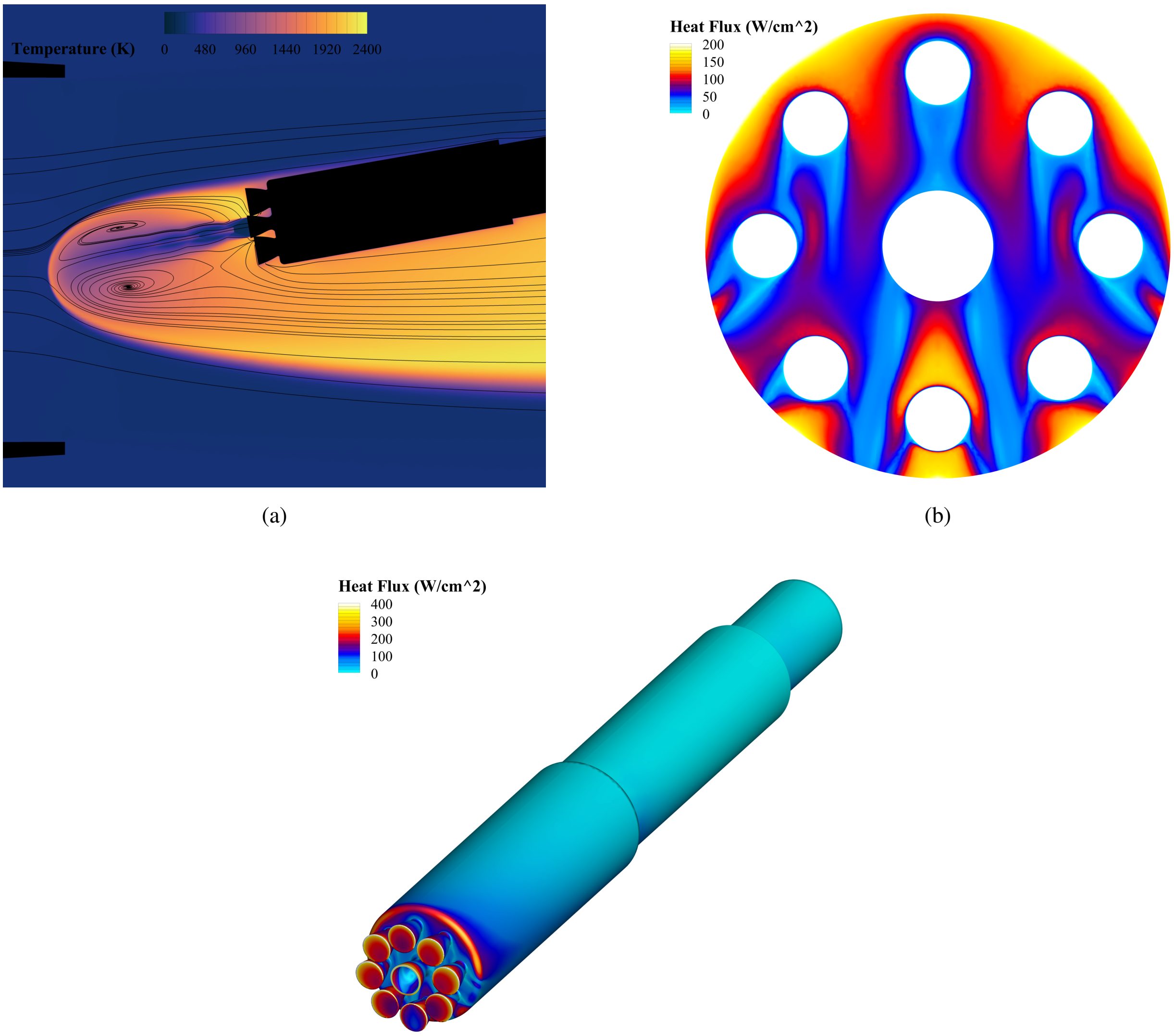

(a) (b) (c)

Figure 10: CFD post processed images showing (a) temperature field with streamlines, (b) baseplate heat flux and (c) heatflux distribution over entire model

5. Conclusions

This paper has presented the results from CFD investigations conducted for the RETPRO VMK test campaign. Given the low O/F ratio, severe post combustion was observed, resulting in high heat loads in the base region. The heat flux distribution was seen to vary significantly according the Mach number and angle of attack. The plume structure was also seen to be sensitive to the grid density. Finally, the base pressure coefficients were found to be sensitive to the combustion chamber temperature, which was estimated using the NASA CEA tool with an equillibrium assumption. Future work will provide comparisons between experimental data and the results presented here for validation of pressure and heat flux values. This will aid in understanding whether the combustion chamber conditions from CEA provides a realistic estimation of the actual enviroment.

References

[1] Tobias Ecker, Sebastian Karl, Etienne Dumont, Sven Stappert, and Daniel Krause. Numerical study on the thermal loads during a supersonic rocket retropropulsion maneuver. *Journal of Spacecraft and Rockets*, 57(1):131–146, 2020.

[2] D. Kirchheck, A. Marwege, J. Klevanski, J. Riehmer, A. Gülhan, S. Karl, and O. Gloth. Validation of wind tunnel test and cfd techniques for retro-propulsion (retpro): Overview on a project within the future launchers preparatory programme (flpp). In *International Conference on Flight Vehicles, Aerothermodynamics and Re-entry Missions and Engineering (FAR)*, October 2019.

[3] M. Laureti and S. Karl. Aerothermal databases and load predictions for retro propulsion-assisted launch vehicles (retalt). *CEAS Space Journal*, January 2022.

[4] J. Klevanski, T. Ecker, J. Riehmer, E. Dumont B. Reimann, and C. Chavagnac. Aerodynamic studies in preparation for callisto - reusable vtvl launcher first stage demonstrator. In *69th International Astronautical Congress*, October 2018.

[5] T. Bykerk, S. Fechter, D. Kirchheck, and S. Karl. Condensation modelling of expanding cold gas jets during hypersonic retro-propulsion manouvres within the retpro project. In *The 23rd Australasian Fluid Mechanics Conference (23AFMC)*, December 2022.

[6] T. Bykerk, D. Kirchheck, and S. Karl. Reconstruction of wind tunnel tests using cfd for a reusable first stage during rocket retro- propulsion. In *9th European Conference for Aeronautics and AeroSpace Sciences (EUCASS)*, July 2022.

[7] M. Ertl, T. Ecker, J. Klevanski amd E. Dumont, and S. Krummen. Aerothermal analysis of plume interaction with deployed landing legs of the callisto vehicle. In *9TH EUROPEAN CONFERENCE FOR AERONAUTICS AND AEROSPACE SCIENCES (EUCASS)*, July 2022.

[8] P. Gerlinger, H. Möbius, and D. Brüggemann. An implicit multigrid method for turbulent combustion. *Journal of Computational Physics*, 2001.